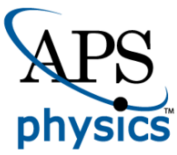

Improved Spatial Resolution Achieved by Chromatic Intensity Interferometry

Lu-Chuan Liu, Luo-Yuan Qu, Cheng Wu, Jordan Cotler, Fei Ma, Ming-Yang Zheng, Xiu-Ping Xie, Yu-Ao Chen, Qiang Zhang, Frank Wilczek, and Jian-Wei Pan

Phys. Rev. Lett. **127**, 103601 — Published 31 August 2021

DOI: 10.1103/PhysRevLett.127.103601

Improved Spatial Resolution Achieved by Chromatic Intensity Interferometry

Lu-Chuan Liu,[1,2,3] Luo-Yuan Qu,[1,2,3,4] Cheng Wu,[1,2,3] Jordan Cotler,[5] Fei Ma,[1,2,3,4] Ming-Yang Zheng,[4] Xiu-Ping Xie,[4] Yu-Ao Chen,[1,2,3] Qiang Zhang,[1,2,3,4] Frank Wilczek,[6,7,8,9,10] and Jian-Wei Pan[1,2,3]

[1]*Hefei National Laboratory for Physical Sciences at the Microscale and Department of Modern Physics, University of Science and Technology of China, Hefei 230026, China*
[2]*Shanghai Branch, CAS Center for Excellence in Quantum Information and Quantum Physics, University of Science and Technology of China, Shanghai 201315, China*
[3]*Shanghai Research Center for Quantum Sciences, Shanghai 201315, China*
[4]*Jinan Institute of Quantum Technology, Jinan, 250101, P. R. China*
[5]*Society of Fellows, Harvard University, Cambridge, MA 02138 USA*
[6]*Center for Theoretical Physics, MIT, Cambridge, MA 02139 USA*
[7]*T. D. Lee Institute, Shanghai Jiao Tong University, Shanghai, 200240, P. R. China*
[8]*Wilczek Quantum Center, School of Physics and Astronomy, Shanghai Jiao Tong University, Shanghai, 200240, P. R. China*
[9]*Department of Physics, Stockholm University, Stockholm SE-106 91 Sweden*
[10]*Department of Physics and Origins Project, Arizona State University, Tempe, AZ 25287 USA*

Interferometers are widely used in imaging technologies to achieve enhanced spatial resolution, but require that the incoming photons be indistinguishable. In previous work, we built and analyzed color erasure detectors which expand the scope of intensity interferometry to accommodate sources of different colors. Here we demonstrate experimentally how color erasure detectors can achieve improved spatial resolution in an imaging task, well beyond the diffraction limit. Utilizing two 10.9 mm-aperture telescopes and a 0.8 m baseline, we measure the distance between a 1063.6 nm source and a 1064.4 nm source separated by 4.2 mm at a distance of 1.43 km, which surpasses the diffraction limit of a single telescope by about 40 times. Moreover, chromatic intensity interferometry allows us to recover the phase of the Fourier transform of the imaged objects – a quantity that is, in the presence of modest noise, inaccessible to conventional intensity interferometry.

Introduction.— Since Hanbury Brown and Twiss (HBT) first proposed an ingenious method to exploit second-order interference [1–3], there has been a revolution in high-resolution imaging. By correlating signals collected by separated detectors, the HBT intensity interferometer can surpass the resolving power of individual detectors in several diverse circumstances. HBT interferometry has been applied in many fields ranging from astronomy to nuclear and elementary particle physics. For example, several large interferometers have demonstrated their superiority in high-resolution imaging of astronomical targets [4–7]. Related methods have also been used successfully to probe nuclear collisions [8], to measure the quantum state of Bose-Einstein condensates [9–13], and to identify complex quantum phases in ultracold bosonic and fermionic atom systems [14–16].

A drawback of conventional interferometric methods is that they only allow interference between photons of the same wavelength. The information encoded in the correlations between photons of different wavelengths has attracted increasing attention in recent years [17–20]. The color erasure detector is a fundamental tool to realize chromatic interferometry [21–23], and recover the hidden information. Unlike previous experiments in chromatic interferometry, which implemented wavelength conversion either at the light sources themselves, or nearby [19, 24–28], our color erasure detectors operate only on photons at the final detection stage. This feature of color erasure detectors allows them to interface smoothly with conventional intensity interferometry [1, 29, 30].

According to the van Cittert-Zernike theorem [31, 32], traditional intensity interferometry only obtains the squared-magnitude of the Fourier transform of the radiance distribution of an imaged object. This loss of phase information poses a severe difficulty in the reconstruction of images. Chromatic intensity interferometry not only achieves interference between sources of different wavelengths, but also obtains the phase of the Fourier transform.

In this paper we demonstrate, theoretically and experimentally, that chromatic intensity interferometry can improve spatial resolution in imaging. In our experiment, we spatially resolve a 1064.4 nm source and a 1063.6 nm source separated by 4.2 mm at a distance of 1.43 km, by measuring the second order correlation of the signal light collected via color erasure detectors.

Theory.— We determine the distance between the light sources as follows. The two sources, labeled S_1 and S_2, are positioned at $\mathbf{r}_1, \mathbf{r}_2$ and emit photons with wavelengths λ_1, λ_2, whose frequency is f_1 and f_2, respectively. Suppose our interferometer consists of two telescopes T_A and T_B positioned at $\mathbf{r}_A$ and $\mathbf{r}_B$, and the photons collected by them are guided to the color erasure detectors [23] A and B, respectively. In each color erasure detector pumped by lasers with frequencies Δf_{31} and Δf_{32}, the received f_1 and f_2 photons are respectively upconverted into color-erased $f_3^{(1)}$ and $f_3^{(2)}$ photons via sum-frequency generation (SFG). After up-conversion, the phase of the pump photon will be added to the signal photon. Mathematically, there are two photon state conversion pro-

cesses

$$|\gamma_{f_1}\rangle \to e^{i\phi_{31}}|\gamma_{f_3^{(1)}}\rangle, \quad |\gamma_{f_2}\rangle \to e^{i\phi_{32}}|\gamma_{f_3^{(2)}}\rangle \tag{1}$$

in each color erasure detector, where ϕ_{31} and ϕ_{32} are the phases of the Δf_{31} and Δf_{32} photons at the detectors, respectively. By analyzing the phases, the electric fields at detectors A and B can be simply described as

$$\begin{aligned} E_A(t) =& |E_{1A}|e^{-2\pi i f_3^{(1)} t + i(\phi_{s_{1A}} + \phi_{f_{1A}} + \phi_{S_1} + \phi_{31A})} \\ &+ |E_{2A}|e^{-2\pi i f_3^{(2)} t + i(\phi_{s_{2A}} + \phi_{f_{2A}} + \phi_{S_2} + \phi_{32A})} \\ E_B(t) =& |E_{1B}|e^{-2\pi i f_3^{(1)} t + i(\phi_{s_{1B}} + \phi_{f_{1B}} + \phi_{S_1} + \phi_{31B})} \\ &+ |E_{2B}|e^{-2\pi i f_3^{(2)} t + i(\phi_{s_{2B}} + \phi_{f_{2B}} + \phi_{S_2} + \phi_{32B})} \end{aligned} \tag{2}$$

In the above formula, $\phi_{s_{1A}}$ represents the phase accumulated due to propagation from S_1 to T_A, $\phi_{f_{1A}}$ is the phase accumulated by the f_1 photon due to propagation in a fiber from T_A to detector A, and so on. The initial phases of S_1, S_2 are ϕ_{S_1}, ϕ_{S_2}. A theoretical formula for the degree of second-order temporal coherence between the light at the two detectors is [23]

$$\begin{aligned} g^{(2)}(\tau) &= \frac{\langle E_B^*(t) E_A^*(t+\tau) E_A(t+\tau) E_B(t)\rangle}{\langle |E_A(t)|^2\rangle \langle |E_B(t)|^2\rangle} \\ &= 1 + \frac{\epsilon}{2}\cos(2\pi(f_3^{(1)} - f_3^{(2)})\tau + \phi_c)\,, \end{aligned} \tag{3}$$

where ϵ is the visibility and ϕ_c is the total phase of the intensity interference. Here $\phi_c = \phi_s + \phi_f + \phi_n$ is the sum of the spatial phase ϕ_s due to spatial propagation from the light sources to the telescopes, the inherent phase ϕ_f due to the optical fibers that carry the pump light or signal light, and the noise phase ϕ_n caused by various factors including atmospheric disturbance and fiber deformation. Note that ϕ_s changes with the positions of the light sources and the telescopes, and its expression is [21]

$$\begin{aligned} \phi_s &= \phi_{s_{1B}} - \phi_{s_{1A}} - \phi_{s_{2B}} + \phi_{s_{2A}} \\ &= \frac{2\pi}{\lambda_1}(|\mathbf{r}_1 - \mathbf{r}_B| - |\mathbf{r}_1 - \mathbf{r}_A|) - \frac{2\pi}{\lambda_2}(|\mathbf{r}_2 - \mathbf{r}_B| - |\mathbf{r}_2 - \mathbf{r}_A|)\,. \end{aligned} \tag{4}$$

Adjusting the direction of the interferometer baseline so that the target falls on its perpendicular bisector, we arrive at the geometry shown in Fig. 1, where x is the distance between the two telescopes, L is the distance from the target to the baseline, d is the projected distance of the two sources onto the baseline, and α is the angle between the perpendicular bisector of the baseline and the midpoint of the two sources. We work in a regime where the parameters satisfy the condition $x/L,\ d/L,\ \alpha \ll 1$. Then specific form of ϕ_s is

$$\phi_s = \frac{2\pi x}{\lambda_h}\left(\theta + \frac{\alpha\Delta\lambda}{\lambda_a}\right), \tag{5}$$

where $\lambda_a = (\lambda_1 + \lambda_2)/2$, $\lambda_h = 2\lambda_1\lambda_2/(\lambda_1 + \lambda_2)$, $\Delta\lambda = \lambda_1 - \lambda_2$, $\theta = d/L$. We can regard ϕ_f as a constant and ϕ_n as a random variable with mean 0. If we ignore ϕ_n and substitute Eqn. (5) into the expression for ϕ_c, we find that $\lambda_h\phi_c/(2\pi)$ is a linear function of x, that is,

$$\frac{\lambda_h\phi_c}{2\pi} = \left(\theta + \frac{\alpha\Delta\lambda}{\lambda_a}\right)x + \text{const.} \tag{6}$$

This shows that if α can be accurately determined, then we can calculate θ from the slope of the $\lambda_h\phi_c/(2\pi)$ vs. x graph and obtain the sought after distance between the light sources. For our purposes, we try to reduce the value of $|\alpha|$, because when $\alpha = 0$, the slope of the $\lambda_h\phi_c/(2\pi)$ vs. x graph is exactly θ, which is more convenient.

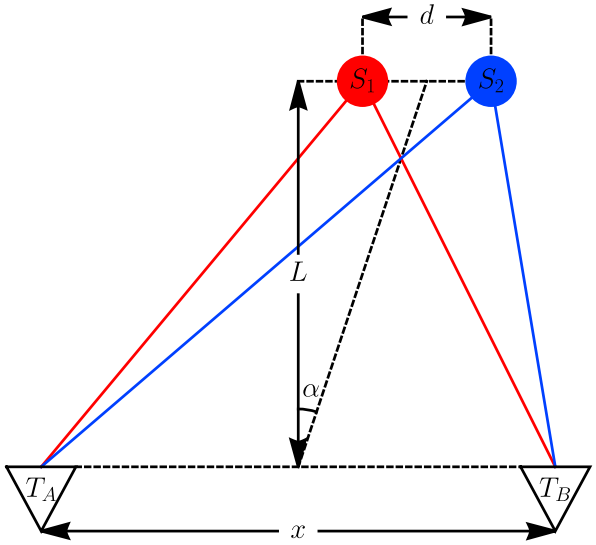

FIG. 1. **Geometry of the intensity interferometer.** Consider a coordinate system with the interferometer baseline and its perpendicular bisector as the axes. Then the telescopes T_A and T_B are positioned at $\mathbf{r}_A = (-x/2, 0)$ and $\mathbf{r}_B = (x/2, 0)$, respectively, and the sources S_1 and S_2 are positioned at $(L\alpha - d/2, L)$ and $(L\alpha + d/2, L)$ in the small angle approximation, respectively.

In the color erasure setting, we can determine ϕ_c as a function of x by measuring $g^{(2)}(\tau)$ for different x, and extract ϕ_c using Eqn. (3). We remark that ϵ is itself a stochastic variable subject to a complicated time-dependent drift. In the standard setting of HBT with sources of the same wavelength, which is equivalent to $f_3^{(1)} = f_3^{(2)}$ in Eqn. (3), $g^{(2)}(\tau)$ becomes $1 + \frac{\epsilon}{2}\cos(\phi_c)$ and it is hard to estimate ϕ_c since the time-dependence of ϵ is difficult to characterize. However, when $f_3^{(1)} \neq f_3^{(2)}$ in the color erasure setting, we can readily extract ϕ_c by examining the dependence of Eqn. (3) on τ, crucially even when the time-dependence of ϵ is complicated.

Experiment.— Next we turn from our theoretical setup to an experimental demonstration of the resolution capabilities of chromatic intensity interferometry. As shown in Fig. 2, in a building $L = 1.43$ km away from our laboratory, a $\lambda_1 = 1063.6$ nm transmission light and a $\lambda_2 = 1064.4$ nm reflected light form two sources separated horizontally by $d = 4.2$ mm.

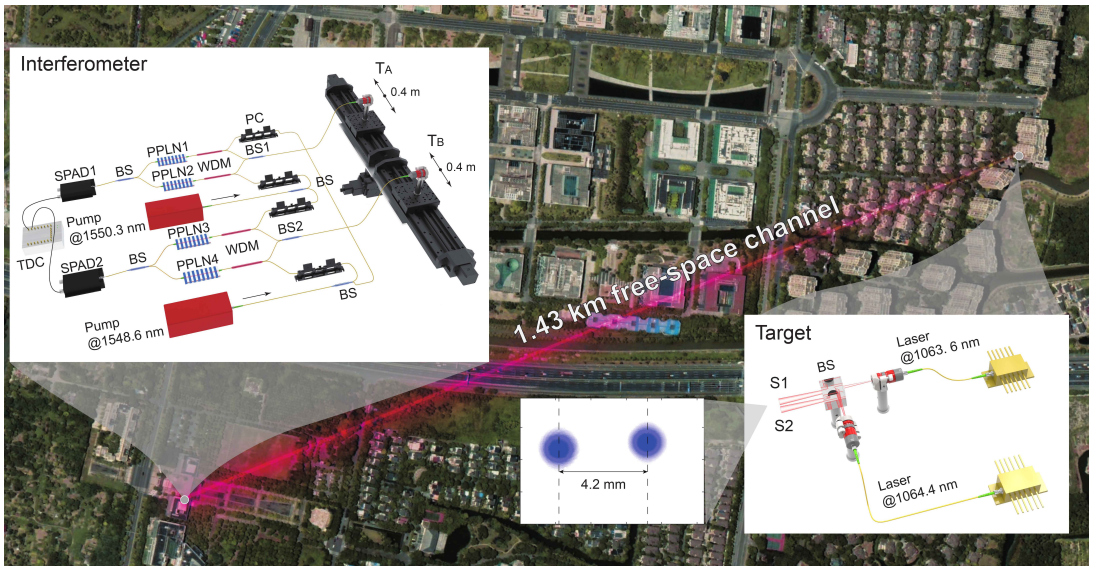

FIG. 2. **Scheme of the chromatic intensity interferometer.** In the 'Target' panel, two sources are coupled to free space by collimators. The 1063.6 nm light passes through the BS and the 1064.4 nm light is reflected, forming two point sources separated by 4.2 mm. The interferometer is 1.43 km away from the target. Two telescopes T_A and T_B move with a translation stage to change the baseline of the interferometer. Photons of different wavelengths collected by T_A (T_B) are divided by BS1 (BS2), and coupled into PPLN1 and PPLN2 (PPLN3 and PPLN4). PPLN1 (PPLN4) is pumped by a 1548.6 nm laser, and PPLN2 (PPLN3) is pumped by a 1550.3 nm laser. The polarization of the pump is controlled by a PC. After the SFG, the upconverted 630.8 nm photons in PPLN1 and PPLN2 (PPLN3 and PPLN4) are combined by BS and guided to SPAD1 (SPAD2). The arrival time of the detected photons is recorded by TDC. By calculating the second order correlation of the signal recorded by TDC with different baselines, we spatially resolve the two sources separated by 4.2 mm at the target. Some abbreviations are: periodically poled lithium niobate waveguide (PPLN), beamsplitter (BS), polarization controller (PC), wavelength division multiplexing (WDM), and Time-Digital Converter (TDC).

The diffraction limit of a single 10.9 mm-aperture telescope is 1.9×10^{-4} rad when $\lambda = 1064$ nm, which means it can only resolve sources separated by more than 0.17 m at a distance of 1.43 km. We utilize chromatic intensity interferometry shown in Fig. 2 to resolve the sources. In our laboratory, two 10.9 mm-aperture telescopes are installed on two 0.4 m-long translation stages, which move symmetrically to change x from 0.16 m to 0.96 m. We place this system on a rotator to adjust the direction of the baseline to satisfy the $\alpha = 0$ condition. Photons collected by each telescope are guided to color erasure detectors of the same design as in [23]. In a pair of parallel PPLN waveguides pumped by 1550.3 nm and 1548.6 nm lasers respectively, the received photons are respectively upconverted into indistinguishable (i.e, $f_3^{(1)} \approx f_3^{(2)}$) 630.8 nm photons via SFG. A time-to-digital converter (TDC) is used to record the arrival time of these photons at two silicon single-photon avalanche diodes (SPAD), from which $g^{(2)}(\tau)$ can be calculated. In order to filter out pump photons and signal photons that have not undergone frequency conversion, we add 631 nm bandpass filters before the two SPADs.

Results.— Taking into account the dark count rate ($\sim$ 1 kHz) and the dead time (22 ns) for the SPADs, we adjust the power and polarization of the pump lasers to control the SFG efficiency in each PPLN so that at different x the counting rate of each SPAD varies from about 1 MHz to 3 MHz. In addition, considering the time resolution capability of the SPADs ($\sim$ 1 ns), when we fine-tune the frequencies of the pump lasers, we only need to make the value of $|f_3^{(1)} - f_3^{(2)}|$ reach on the order of 10 MHz. Fig. 3(a) shows the result of performing a $g^{(2)}(\tau)$ measurement at $x = 0.16$ m calculated from the 0.5 s of photon arrival events using a 5 ns time bin. We set the software time delay so that τ ranges from -0.5 μs to 0.5 μs, and its corresponding optimized fitting parameters are $f_3^{(1)} - f_3^{(2)} = 15.79 \pm 0.01$ MHz and $\epsilon = 0.274 \pm 0.06$. After this step of preparation, we let the two telescopes reciprocate symmetrically on the two translation stages, changing x at a speed of 0.05 m/s, and at the same time we continuously perform the $g^{(2)}(\tau)$ measurement with the same optimized parameters. That is to say, after every 0.5 s, when x changes by 0.025 m, a fitted value of ϕ_c is obtained. Each time the telescopes move from one end of the translation stages to the other, we obtain a data set of $\lambda_h \phi_c/(2\pi)$ as a function of x on the entire baseline and linearly fit the slope θ, as shown in Fig. 3(b). We repeat this kind of θ measurement 10 times and plot all the results in Fig. 3(c). The experimental average $\bar{\theta}$ and the experimental standard deviation of the average $s(\bar{\theta})$ are

$$\bar{\theta} = 3.7 \times 10^{-6} \text{ rad}, \quad s(\bar{\theta}) = 2.5 \times 10^{-7} \text{ rad}. \tag{7}$$

The experimental error of θ here has two main factors; we will evaluate the uncertainties caused by each factor separately and then combine them. First, the value of ϕ_n drifts

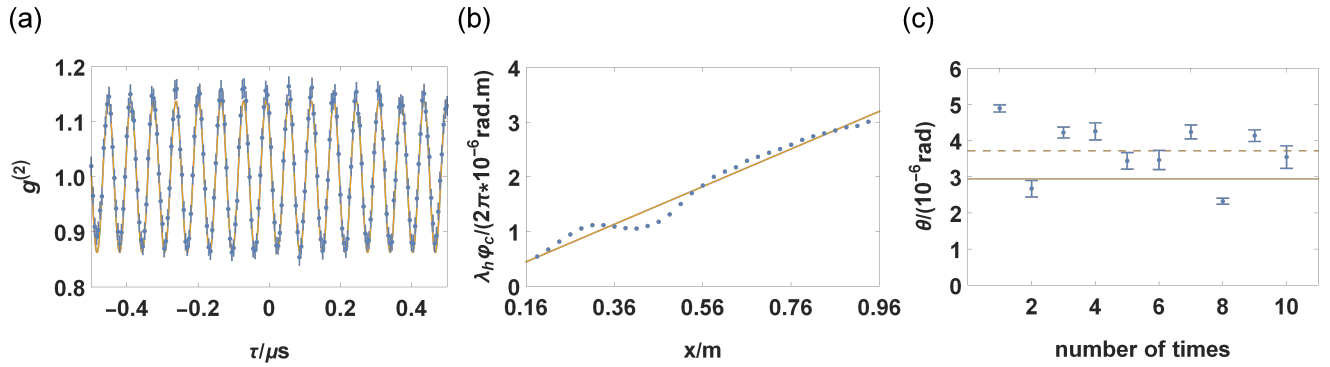

FIG. 3. **Experimental data for the chromatic intensity interferometer.** (a) A plot of the $g^{(2)}(\tau)$ measurement at $x = 0.16$ m with optimized parameters. The orange curve is a least squares fit to the measured data (blue dots). (b) A graph of $\lambda_h\phi_c/(2\pi)$ as a function of x on the entire baseline. The orange line is a least squares fit to the measured data (blue dots). The slope of the fitted line provides a measurement of θ. This set of data corresponds to the 5th point in the next panel. (c) Shown are 10 measurements of θ and their distribution. The vertical position of the orange solid line is the actual value of θ, and the vertical position of the orange dashed line is the average of these measurements (blue dots).

randomly over time, which causes random errors in the ϕ_c measurement whenever the telescope moves along the baseline. This is a Type A uncertainty that can be evaluated by statistical methods. Regarding multiple repeated measurements as a complete θ measurement, the Type A standard uncertainty $u_A(\theta)$ can be evaluated as the experimental standard deviation of the average, that is, $u_A(\theta) = s(\bar{\theta})$.

Second, the systematic error in the measurement and the adjustment of various angle parameters in the experimental system will lead to uncertainty for the α measurements, which is quantified as a standard uncertainty $u(\alpha)$. According to Eqn. (6), the actual fitting parameter in our experiment is $\theta + \frac{\alpha\Delta\lambda}{\lambda_a}$, so $u(\alpha)$ will result in a Type B standard uncertainty $u_B(\theta)$, which has the form $u_B(\theta) = \frac{|\Delta\lambda|}{\lambda_a}u(\alpha = 0)$.

For our experimental system, $u(\alpha)$ is mainly determined by the angle adjustment error of the rotator. The rotator can drive the gear through a stepper motor to rotate the translation stage by a minimum of about 1×10^{-3} rad each time. We use a rectangular distribution with a half-width of 1×10^{-3} rad to evaluate $u(\alpha = 0) = \frac{1}{\sqrt{3}} \times 10^{-3}$ rad. Finally, we calculate the combined standard uncertainty $u_C(\theta)$ as

$$\begin{aligned} u_C(\theta) &= \sqrt{u_A^2(\theta) + u_B^2(\theta)} \\ &= \sqrt{s^2(\bar{\theta}) + \left(\frac{\Delta\lambda}{\lambda_a}\right)^2 u^2(\alpha = 0)}. \\ &= 5.0 \times 10^{-7} \text{ rad}. \end{aligned} \tag{8}$$

The actual value of θ is $d/L = 2.93 \times 10^{-6}$ rad, which falls within two standard deviations of the experimental result. This result shows that the two light sources at the target are successfully resolved, indicating that our interferometer can measure an angular distance which surpasses the diffraction limit of a single telescope by about 40 times.

As a summary, in our work, we demonstrate the capability of chromatic intensity interferometry to achieve enhanced spatial resolution in a regime where existing imaging techniques fail. The main advantages of our scheme are that it expands the range of intensity interferometry to the multi-wavelength setting and gives us access to the phase of the Fourier transform of the imaged objects.

Discussion.— To further improve spatial resolution, chromatic intensity interferometers should be carefully designed to eliminate the internal phase noise, and $\Delta\alpha$ should be pushed as low as possible. If we can further suppress the phase noise and increase the number of repeated measurements, the fitting of $\lambda_h\phi_c/(2\pi)$ as a function of x will become more accurate. This will result in a decrease in $u_A(\theta)$, which would enable the interferometer to achieve a higher spatial resolution. Equivalently, a low signal-to-noise ratio would make ϕ_c more sensitive to small changes in x, so that the same level of spatial resolution could be achieved with a shorter baseline and fewer repeated measurements.

However, $u_B(\theta)$ cannot experimentally be reduced by using a longer baseline and performing more repeated measurements. Theoretically, the spatial resolution limit $\Delta\theta$ of the chromatic intensity interferometer when $u_A(\theta) = 0$ has the form $\Delta\theta = \frac{|\Delta\lambda|}{\lambda_a}\Delta\alpha$, where $\Delta\alpha$ generally represents the accuracy of targeting. In this case, $\Delta\alpha$ depends on the optical limit of the system. If we use a telescope with an aperture of diameter D to measure the direction of a distant unknown target, the accuracy will be at the order of $\frac{\lambda}{D}$. In the case of $|\Delta\lambda| \ll \lambda_a$, we have $\lambda_1 \approx \lambda_2 \approx \lambda_a = \lambda$. Then an estimate of the spatial resolution limit is $\Delta\theta \sim \frac{|\Delta\lambda|}{D}$.

In the coming future, with the development of high-precision time-frequency transmission [33], long-baseline intensity interferometry [34] will realize its advantage over other methods. If combined with telescope arrays [7, 35, 36], color erasure detectors could help with the detection of astronomical targets with nontrivial color distributions or varying

doppler shifts [37]. For laser illumination imaging of space objects [38, 39], if we illuminate space debris with lasers of different colors and utilize color erasure detectors, it may be possible to reconstruct features of the target which are otherwise inaccessible using other methods.

Acknowledgements This work was supported by the National Key R&D Program of China (No.2018YFB0504300),the National Natural Science Foundation of China, the Chinese Academy of Sciences (CAS), Shanghai Municipal Science and Technology Major Project (Grant No.2019SHZDZX), and Anhui Initiative in Quantum Information Technologies. JC is supported by a Junior Fellowship from the Harvard Society of Fellows and the U.S. Department of Energy under grant Contract Number DE-SC0012567. FW's work is supported by the U.S. Department of Energy under grant Contract Number DE-SC0012567, by the European Research Council under grant 742104, and by the Swedish Research Council under Contract No. 335-2014-7424.

[1] R. H. Brown and R. Twiss, Nature **178**, 1046 (1956).
[2] R. H. Brown and R. Q. Twiss, Proceedings of the Royal Society of London. Series A. Mathematical and Physical Sciences **242**, 300 (1957).
[3] R. H. Brown, *The intensity interferometer; its application to astronomy* (London, Taylor & Francis; New York, Halsted Press, 1974).
[4] R. Hanbury Brown, J. Davis, L. Allen, and J. Rome, Monthly Notices of the Royal Astronomical Society **137**, 393 (1967).
[5] J. E. Baldwin, R. C. Boysen, C. A. Haniff, P. R. Lawson, C. D. Mackay, J. Rogers, D. Saint-Jacques, P. J. Warner, D. M. Wilson, and J. S. Young, in *Astronomical Interferometry*, Vol. 3350 (International Society for Optics and Photonics, 1998) pp. 736–745.
[6] J. Davis, W. Tango, A. Booth, E. Thorvaldson, and J. Giovannis, Monthly Notices of the Royal Astronomical Society **303**, 783 (1999).
[7] A. Abeysekara, W. Benbow, A. Brill, J. Buckley, J. Christiansen, A. Chromey, M. Daniel, J. Davis, A. Falcone, Q. Feng, *et al.*, Nature Astronomy , 1 (2020).
[8] G. Baym, Acta Phys. Polon. B **29**, 1839 (1998), nucl-th/9804026.
[9] S. Fölling, F. Gerbier, A. Widera, O. Mandel, T. Gericke, and I. Bloch, Nature **434**, 481 (2005).
[10] M. Schellekens, R. Hoppeler, A. Perrin, J. V. Gomes, D. Boiron, A. Aspect, and C. I. Westbrook, Science **310**, 648 (2005).
[11] A. Öttl, S. Ritter, M. Köhl, and T. Esslinger, Physical Review Letters **95**, 090404 (2005).
[12] A. Polkovnikov, E. Altman, and E. Demler, Proceedings of the National Academy of Sciences **103**, 6125 (2006).
[13] H. Cayla, S. Butera, C. Carcy, A. Tenart, G. Hercé, M. Mancini, A. Aspect, I. Carusotto, and D. Clément, Physical Review Letters **125**, 165301 (2020).
[14] M. Henny, S. Oberholzer, C. Strunk, T. Heinzel, K. Ensslin, M. Holland, and C. Schönenberger, Science **284**, 296 (1999).
[15] T. Jeltes, J. M. McNamara, W. Hogervorst, W. Vassen, V. Krachmalnicoff, M. Schellekens, A. Perrin, H. Chang, D. Boiron, A. Aspect, *et al.*, Nature **445**, 402 (2007).
[16] R. Dall, A. Manning, S. Hodgman, W. RuGway, K. V. Kheruntsyan, and A. Truscott, Nature Physics **9**, 341 (2013).
[17] J. Cotler and F. Wilczek, arXiv preprint arXiv:1502.02477 (2015).
[18] H.-H. Lu, J. M. Lukens, N. A. Peters, O. D. Odele, D. E. Leaird, A. M. Weiner, and P. Lougovski, Physical Review Letters **120**, 030502 (2018).
[19] H.-H. Lu, J. M. Lukens, N. A. Peters, B. P. Williams, A. M. Weiner, and P. Lougovski, Optica **5**, 1455 (2018).
[20] M. Kues, C. Reimer, J. M. Lukens, W. J. Munro, A. M. Weiner, D. J. Moss, and R. Morandotti, Nature Photonics **13**, 170 (2019).
[21] J. Cotler, F. Wilczek, and V. Borish, arXiv preprint arXiv:1607.05719 (2016).
[22] L.-Y. Qu, J. Cotler, F. Ma, J.-Y. Guan, M.-Y. Zheng, X. Xie, Y.-A. Chen, Q. Zhang, F. Wilczek, and J.-W. Pan, Physical Review Letters **123**, 243601 (2019).
[23] L.-Y. Qu, L.-C. Liu, J. Cotler, F. Ma, J.-Y. Guan, M.-Y. Zheng, Q. Yao, X. Xie, Y.-A. Chen, Q. Zhang, *et al.*, Optics Express **28**, 32294 (2020).
[24] H. Takesue, Physical review letters **101**, 173901 (2008).
[25] M. Raymer, S. Van Enk, C. McKinstrie, and H. McGuinness, Optics Communications **283**, 747 (2010).
[26] K. De Greve, L. Yu, P. L. McMahon, J. S. Pelc, C. M. Natarajan, N. Y. Kim, E. Abe, S. Maier, C. Schneider, M. Kamp, and S. Hfling, Nature **491**, 421 (2012).
[27] T. Kobayashi, R. Ikuta, S. Yasui, S. Miki, T. Yamashita, H. Terai, T. Yamamoto, M. Koashi, and N. Imoto, Nature photonics **10**, 441 (2016).
[28] T. Kobayashi, D. Yamazaki, K. Matsuki, R. Ikuta, S. Miki, T. Yamashita, H. Terai, T. Yamamoto, M. Koashi, and N. Imoto, Optics Express **25**, 12052 (2017).
[29] R. Twiss and R. H. Brown, Nature **179**, 1128 (1957).
[30] G. Baym, Acta Physica Polonica. Series B **29**, 1839 (1998).
[31] P. H. van Cittert, Physica **1**, 201 (1934).
[32] F. Zernike, Physica **5**, 785 (1938).
[33] Q. Shen, J.-Y. Guan, T. Zeng, Q.-M. Lu, L. Huang, Y. Cao, J.-P. Chen, T.-Q. Tao, J.-C. Wu, L. Hou, *et al.*, arXiv preprint arXiv:2003.08322 (2020).
[34] D. Dravins, in *Optical and Infrared Interferometry and Imaging V*, Vol. 9907 (International Society for Optics and Photonics, 2016) p. 99070M.
[35] P. D. Nunez, R. Holmes, D. Kieda, and S. LeBohec, Monthly Notices of the Royal Astronomical Society **419**, 172 (2012).
[36] D. Kieda and N. Matthews, arXiv preprint arXiv:1709.03956 (2017).
[37] I. K. Baldry, K. Glazebrook, J. Brinkmann, Ž. Ivezić, R. H. Lupton, R. C. Nichol, and A. S. Szalay, The Astrophysical Journal **600**, 681 (2004).
[38] D. G. Voelz, S. D. O'Keefe, J. D. Gonglewski, D. B. Rider, and K. J. Schulze, in *Optics in Atmospheric Propagation and Random Phenomena*, Vol. 2312 (International Society for Optics and Photonics, 1994) pp. 202–211.
[39] E. L. Cuellar, J. Cooper, J. Mathis, and P. Fairchild, in *Unconventional Imaging IV*, Vol. 7094 (International Society for Optics and Photonics, 2008) p. 70940G.